Modeling lithium diffusion in battery cathodes considering chemo-mechanically induced damage

Jeffery M. Allen[a], Peter J. Weddle[b], Ankit Verma[b], Anudeep Mallarapu[b], Francois Usseglio-Viretta[b], Donal P. Finegan[b], Andrew M. Colclasure[b], Weijie Mai[b], Volker Schmidt[c], Orkun Furat[c], David Diercks[d], Tanvir Tanim[e], Kandler Smith[b]

Question/Comments? Contact: Jeff.allen@nrel.gov

[a]Computational Science Center, National Renewable Energy Laboratory, Golden, CO 80401, USA
[b]Energy Conversion & Storage Systems, National Renewable Energy Laboratory, Golden, CO 80401, USA
[c]Institute of Stochastics, Ulm University, D-89060 Ulm, Germany
[d]Materials Science Program, Colorado School of Mines, Golden, CO 80401, USA
[e]Idaho National Laboratory, 2525 N. Fremont, Idaho Falls, ID 83415, USA

Background

A Li-ion battery has two electrodes, the anode and the cathode, with electrolyte percolating between them. When cycling, the battery can lose capacity. Diagnosing reasons for this capacity loss and developing design/control strategies to address this capacity loss is of great interest.

One possible source of capacity loss is cathode degradation. The cathode is composed of numerous secondary particles bound together by electrolytically conductive carbon-binder. These secondary particles are made of smaller primary particles commonly referred to as grains.

The goal of this study is to develop a continuum-damage model that investigates conditions that can lead to NMC532 (cathode) secondary particles degradation. The conditions studied here are the charge rate, secondary particle size, and primary particle size. The continuum model is written in such a way to improve computational speed and efficiency.

Continuum Damage Electro-Mechanical Model

Lithium Transport:

$$\frac{\partial c_s}{\partial t} = -\nabla \cdot N_s, \qquad N_s = -D_s \nabla c_s$$

Diffusion (D_s); Lithium concentration (c_s)

Solid-Phase Potential:

$$0 = -\nabla \cdot j_s, \qquad j_s = -\kappa_s \nabla \phi_s$$

Conductivity (κ_s); Potential (ϕ_s)

Mechanics:

$$\nabla \cdot \sigma = 0, \qquad \sigma = C[\varepsilon - \beta \Delta c_s], \qquad \varepsilon = \frac{1}{2}\left(\nabla u + (\nabla u)^T\right)$$

Stress tensor (σ); Expansion tensor (β); Stiffness tensor (C); Strain-rate tensor (ε); Displacement (u)

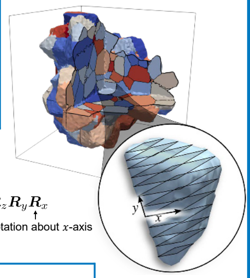
Crystal Orientation

Anisotropy:

$$D_s \to -\boldsymbol{R} \boldsymbol{D}_s \boldsymbol{R}^{-1}, \qquad \boldsymbol{D}_s = \begin{bmatrix} s_{xy} & 0 & 0 \\ 0 & s_{xy} & 0 \\ 0 & 0 & s_z \end{bmatrix} D_s, \qquad \boldsymbol{R} = \boldsymbol{R}_z \boldsymbol{R}_y \boldsymbol{R}_x$$

Diffusion tensor; In-plane scaling (s_{xy}); Through-plane scaling (s_z); Rotation Matrix ($\boldsymbol{R}$); Rotation about x-axis ($\boldsymbol{R}_x$)

Damage Factor:

$$D = \begin{cases} 0 & \text{if } \varepsilon^e_{eq} < k_i \\ \frac{k_f}{\varepsilon^e_{eq}} \frac{\varepsilon^e_{eq} - k_i}{k_f - k_i} & \text{if } k_i < \varepsilon^e_{eq} < k_f \\ 1 & \text{if } \varepsilon^e_{eq} > k_f \end{cases}, \qquad \varepsilon^e_{eq} = \sqrt{\sum_{i=1}^{3} (< \varepsilon^e_i >)^2}$$

Damage Factor (D); Crack initiation (k_i); Loss of integrity (k_f); Equivalent strain (ε^e_{eq})

$$D_{n+1} = \max\left(\{D, D_n\}\right), \qquad \hat{C} = \max\left(\{(1-D), 0.1\}\right) C, \qquad \hat{\mathbf{D}}_s = (1-D)\mathbf{D}_s$$

Damaged regions cannot recover; Stiffness reduced with damage; Diffusion halted

Boundary Conditions:

$$j_s \cdot \vec{n} = I_{app} F, \qquad \phi_s = \phi_{cv}$$

Applied current (I_{app}), Constant current; Cut-off voltage (ϕ_{cv}), Constant voltage

$$N_s \cdot \vec{n} = \frac{i_{se}}{F}, \qquad j_s \cdot \vec{n} = i_{se}, \qquad i_{se} = 2 i_0 \sinh\left(\frac{F\eta}{2RT}\right), \qquad \eta = \phi_s - \phi_e - U_0$$

Surface electrochemical reaction; Current density (i_{se}); Butler-Volmer; Electrolyte potential (fixed) (ϕ_e); Overpotential (η); Equilibrium potential (U_0)

Note: The charge rate (used to calculate I_{app}), is the current required to completely charge a particle in one hour, usually denoted: 1C. A C-rate of 6C is the current required to charge in a sixth of an hour and C/2 charges in 2 hours.

Geometries

This study investigated 5 different geometries that varied in both secondary particle size and grain size. These geometries were constructed using a statistically inform algorithm from from Furat et al. [1].

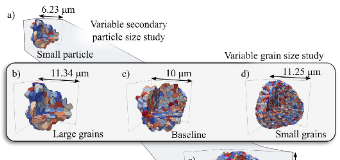

Secondary-particle name	Figure reference	Particle volume (μm^3)	Particle diameter (μm)	Number of grains	Average grain volume (μm^3)	Standard deviation grain volume (μm^3)
Small particle	(a)	80.8	6.23	152	5.32E−1	3.99E−1
Large grains	(b)	487	11.34	152	3.20E+0	2.40E+0
Baseline	(c)	487	10	916	5.32E−1	4.11E−1
Small grains	(d)	487	11.25	6095	7.99E−2	6.13E−2
Large particle	(e)	3240	21.16	6095	5.32E−1	4.08E−1

Simulation Setup

All simulations are ran using a Python package built on the FEniCS project [2]. The meshes were around 800k degrees of freedom for the electro-mechanical system and a single charge/discharge cycle ran in ~1 hr 40 min on 72 processors.

Four sets of charge conditions are demanded per Geometry. Before cycling, a formation procedure is simulated consisting of three, C/10 cycles followed by an additional three, C/2 cycles. After formation, each particle is cycled an additional 25 times at 1C, 4C, 6C, and 9C charging for 60, 15, 10, and 10 minutes, respectively. The constant-current constant-voltage charge has a cut-off voltage of 4.2 V. Particles are then discharged at a C/2 rate until 3.4 V. Reference performance tests (RPT) of C/20 charge/discharge are simulated after formation and after 25 cycles for each condition. The RPT discharge capacities are compared to determine cathode capacity fade. Below are results for the Baseline Geometry after 25 cycles.

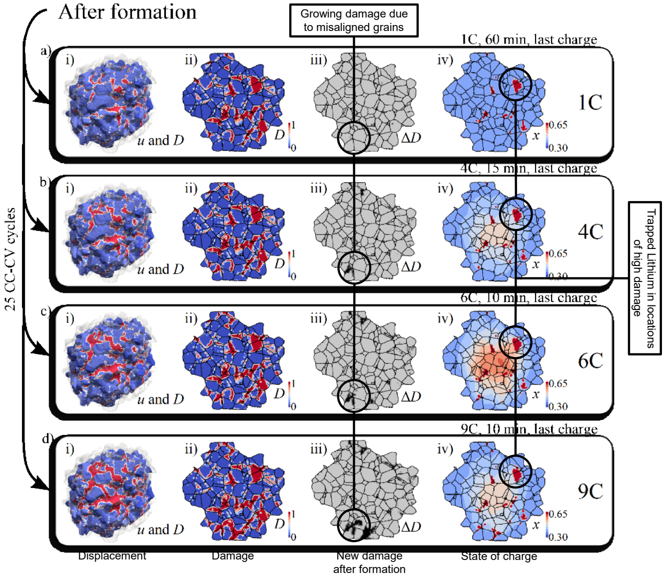

Validation

A few parameters needed to be determined. (right) The diffusion coefficient was scaled to match voltage curves from Colclasure et al. [3]. (left) The crack initiation, k_i, was determined by comparing capacity loss from Baseline simulations to experimental result from Tanim et al. [39].

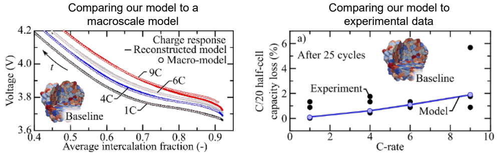

Results

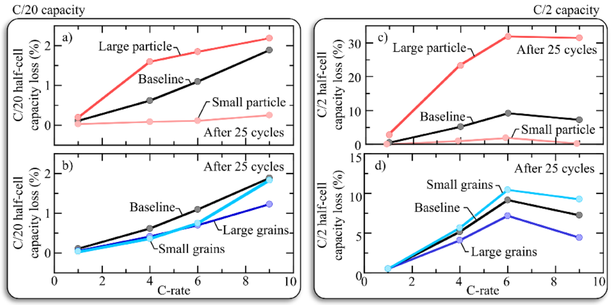

Above are results from all simulations. The left column computed capacity loss by comparing the C/20 discharge capacity after formation and after 25 cycles. The right column is the same calculation but using a C/2 rate. Parts a) and c) compare the geometries with varying secondary particle size and b) and d) compare the geometries with varying grains.

For the secondary particle size study, the smaller particle performs better in terms of capacity retention regardless charge rate. The larger particles have worse capacity retention due to the relatively longer diffusion lengths, which result in larger concentration gradients resulting in increased stress/damage.

For grain size study, the trend is less obvious. When comparing C/20 discharge times in b), there seems to be no preference between small and large grains. However, for C/2 in d) there is a slight preference for large grains. This is because at slow charge rates, the mismatch of grain orientation does not significantly hinder diffusion, but at faster charge rates, Li must take more tortuous paths through the mismatch grains to reach the center. This results in longer effective diffusion lengths for geometries with smaller grains.

Conclusions

Damage/capacity loss seems to be strongly tied to the effective diffusion length of the secondary particle geometry. Because of this, smaller NMC532 secondary particles with large grains experience less capacity loss due to chemo-mechanical effects.

References

[1] O. Furat, L. Petrich, D. Diercks, F. Usseglio-Viretta, K. Smith, and V. Schmidt. *Artificial generation of representative single Li-ion electrode particle architectures from microscopy data.* npj Comput. Mat., Preprint (submitted), 2021.
[2] A. Logg, K. A. Mardal, and G. N. Wells. *Automated Solution of Differential Equations by the Finite Element Method.* Springer, 2012.
[3] T. R. Tanim, Z. Yang, A. M. Colclasure, P. R. Chinnam, P. Gasper, S. B. Son, P. J. Weddle, E. J. Dufek, I. Bloom, K. Smith, C. C. Dickerson, M. C. Evans, A. R. Dunlop, S. E. Trask, B. J. Polzin, and A. N. Jansen. *Extended cycle life implications of fast charging for lithium-ion battery cathode.* Preprint (submitted), 2021.
[4] A. M. Colclasure, T. R. Tanim, A. N. Jansen, S. E. Trask, A. R. Dunlop, B. J. Polzin, D. Robertson, L. Flores, M. Evans, E. J. Dufek, and K. Smith. *Electrode scale and electrolyte trans-port effects on extreme fast charging of lithium-ion cells.* Electrochem. Acta, 2020.

This work is authored in part by the National Renewable Energy Laboratory, operated by Alliance for Sustainable Energy, LLC, for the U.S. Department of Energy (DOE) under Contract No. DE-AC36-08GO28308, and in part by Idaho National Lab, operated by Battelle Energy Alliance for the U.S. Department of Energy under contract DE-AC07-05ID14517. Funding is provided by the U.S. DOE Office of Vehicle Technology Energy Storage Program, eXtreme Fast Charge and Cell Evaluation of Lithium-Ion Batteris (XCEL) Program, program manager Samuel Gillard. The views expressed in the article do not necessarily represent the views of the DOE or the U.S. Government.

InterPore2021 Online Conference
13th Annual Meeting
31 May – 4 June2021
NREL/PO-2C00-80050